

# Functionalization of ceramic tile surface by soluble salts addition: Part I

Federica Bondioli<sup>a,\*</sup>, Tiziano Manfredini<sup>a</sup>, Michele Giorgi<sup>b</sup>, Graziano Vignali<sup>b</sup>

<sup>a</sup> *Università di Modena e Reggio Emilia, Dipartimento di Ingegneria dei Materiali e dell'Ambiente, Via Vignolese 905, 41100 Modena, Italy*

<sup>b</sup> *METCO srl, Via Galileo Galilei 53, Montevoglio (BO), Italy*

Received 15 May 2009; received in revised form 29 July 2009; accepted 13 August 2009

Available online 6 September 2009

## Abstract

The aim of this investigation was the surface functionalization of industrial ceramic tiles by soluble salts addition to improve mechanical properties (resistance to scratch and wear) preserving the aesthetical aspect of the final product. This objective was pursued through the application of different solution of zirconium capable to be transformed in zirconia nanoparticles during the material sintering. The solutions, in different concentrations, were deposited (300 g/m<sup>2</sup>) on unglazed green tiles by air-brushing. The obtained products were polished and characterized in terms of microstructure, surface micromechanical and technological properties based on the UNI EN ISO reference rules. The final aesthetical aspect of the products and the obtained hue variation were evaluated by means of UV–vis spectroscopy and colorimetric analysis.

© 2009 Elsevier Ltd. All rights reserved.

**Keywords:** Functionalization; Tile; Zirconia; Scratch resistance

## 1. Introduction

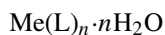
The unglazed fine porcelainized stoneware tile, also called porcelainized stoneware or grés, is a product used both for internal and external applications in building field. Low-porosity, high mechanical, abrasion, chemical and stain resistance make this material ideal to flooring areas with elevated public use.<sup>1,2</sup> Its high technical properties are mainly due to an extremely sintered body composed of different crystalline phases (anorthite, mullite and quartz) immersed in a vitreous matrix.<sup>3,4</sup> In the ceramic tiles industrial field, the porcelainized tiles have become more and more important with regard to its spread from very few market shares limited as to their application fields to more and more diversified ones; the result has been a clear increase in production volumes. This product, which was formerly considered only from a technical standpoint, nowadays shows high aesthetical potentialities allowing its use for over-refined purposes. In particular, the surface hardness of the unglazed porcelainized tiles allows mirror-polished surfaces that give to this product a high aesthetical quality. The main problem is that this material, even if it has a very low open porosity (about 0.1% as to the absorbed water, and 0.5% according to

the mercury porosimetry), has an internal closed porosity of around 6%, with pore sizes range from 1 to 10 µm. This porosity appears during the polishing phase, where about 0.5–1 mm of the superficial layer is removed, causing a superficial microporosity that increases the tendency to the product dirtiness. There are many ways of intervention (some of them have already been widely adopted) as for example using transparent polymeric layers, however the mechanical properties and chemical durability of these coatings are often very poor.<sup>5</sup> The development of functionalized surfaces has recently been under the focus of nanotechnology, i.e. by investigating self-cleaning surface using TiO<sub>2</sub> nanoparticles.<sup>6–10</sup> For example, in a recent work, the authors reported the possibility of surface functionalization of industrial ceramic tiles by sol–gel technique to improve both wear resistance and cleanability of unglazed surfaces.<sup>11</sup> TiO<sub>2</sub>–SiO<sub>2</sub> binary films were deposited by air-brushing on fired tiles obtaining a photocatalytically active building materials, a self-cleaning and self-sterilizing surface that, moreover, might degrade several organic contaminants in the surrounding environment by UV radiation activation.

One of the main interesting properties of nanoparticles, characterized by a mean diameter below the light wavelength, is their transparency if applied on a substrate or dispersed in a matrix. To take advantage of this property, the aim of this study was oriented in the application of different solution of zirconium capable to be transformed in zirconia nanoparticles

\* Corresponding author. Tel.: +39 059 205 6242; fax: +39 059 205 6243.  
E-mail address: [federica.bondioli@unimore.it](mailto:federica.bondioli@unimore.it) (F. Bondioli).

during the material sintering. The goal was the obtainment of a surface with a higher sinterisation degree with respect to the ceramic body. Over the years, zirconium oxide ( $\text{ZrO}_2$ ) has been largely used because of its chemical and physical properties, such as excellent chemical resistance, high refractoriness, wear resistance and hardness. In this work to improve mechanical properties preserving the aesthetical aspect of the final product, four different zirconium-based solution were applied by air-brushing on ceramic tiles before the sinterisation step. The idea is not different from that of “soluble salts”, the conventional name used for new products for coloring unglazed ceramic materials. Originally developed as an alternative to conventional coloring with solid pigments, soluble salts are aqueous solutions of organic complexes of chromophore metals. These solutions are able to color the surface layer of ceramic material and due to their properties of penetration and diffusion, they reach a depth of several mm, making it possible to polish finished products without affecting the decoration. Soluble salts can be represented by the following generic formula:



where Me is the metallic ion and L the complexing agent, generally an organic derivate that is completely decomposed into non-hazardous products, such as  $\text{CO}_2$  and  $\text{H}_2\text{O}$ , during the ceramic firing. In this work, the chromophore ion was substituted by zirconium and four different soluble salts were designed and developed. The obtained solutions, in different concentrations, were deposited ( $300 \text{ g/m}^2$ ) on unglazed green tiles. After an industrial thermal treatment, the obtained products were polished and characterized in terms of microstructure, surface micromechanical and technological properties based on the UNI EN ISO reference rules. The final aesthetical aspect of the products and the obtained hue variation were evaluated by means of UV–vis spectroscopy and colorimetric analysis.

## 2. Experimental

### 2.1. Solution preparation and application

Zirconium solutions were especially prepared by METCO and referred as sol  $\text{ZrX}_n\text{Y}$  where X is the counter ion type used

and Y is the dilution performed. The starting solution, in fact, was diluted up to 5 times in order to evaluate the best conditions in terms of penetration and mechanical properties. I.e. Y is equal to 0 when the solution was used as received, equal to 5 when the solution is diluted 5 times. Table 1 lists in detail the zirconium content in the starting solutions.

The application of sols was performed by air-brushing<sup>12</sup> on unglazed green tiles. To obtain a laboratory scale tile, the atomized powder with a common composition for porcelainized stoneware, kindly provided by Marazzi Group, I, was uniaxially pressed at 40 MPa to produce round samples (40 mm diameter, 5 mm thickness). The deposition technique was chosen, on a laboratory scale, taking into account the industrial applicability and the possible technological solutions necessary to implement these surface treatments in the industrial traditional process. During the air-brushing application, the substrates were kept at a distance of about 14 cm from the air-brush applicator. Each sample was coated with  $300 \text{ g/m}^2$  of solution. After this treatment, the compacts were dried at  $105^\circ\text{C}$  up to constant weight and then fired in a semi-industrial kiln at  $T_{\text{max}} 1210^\circ\text{C}$  with a cycle of 60 min. All the obtained samples were also polished in order to obtain mirror-polished surfaces removing 0.5 mm of superficial layer.

### 2.2. Tile characterizations

The densification obtained after the sintering step was described in terms of water absorption, as required by UNI EN ISO 10545.3, together with linear shrinkage. The effect of zirconia on the tile color was determined by performing color measurements on both untreated and treated tiles by UV–Vis spectroscopy (model Lambda 19, Perkin Elmer) using the CIELab method in order to obtain  $L^*$ ,  $a^*$  and  $b^*$  values.<sup>13</sup> The method defines a color through three parameters,  $L^*$ ,  $a^*$ , and  $b^*$ , measuring brightness, red/green and yellow/blue color intensities, respectively.<sup>14</sup> The method allows, moreover, to define a color difference as  $\Delta E^*$ , based on the relationship:

$$\Delta E^* = [(\Delta L^*)^2 + (\Delta a^*)^2 + (\Delta b^*)^2]^{1/2} \quad (1)$$

Table 1  
Chemical composition of the prepared solutions.

| Commercial name | Sample code | Zr content (wt%) | Commercial name | Sample code | Zr content (wt%) |
|-----------------|-------------|------------------|-----------------|-------------|------------------|
| F108            | Zr1_0       | 7.4              | F335            | Zr2_0       | 7.4              |
|                 | Zr1_1       | 3.7              |                 | Zr2_1       | 3.7              |
|                 | Zr1_2       | 1.85             |                 | Zr2_2       | 1.85             |
|                 | Zr1_3       | 0.93             |                 | Zr2_3       | 0.93             |
|                 | Zr1_4       | 0.46             |                 | Zr2_4       | 0.46             |
|                 | Zr1_5       | 0.23             |                 | Zr2_5       | 0.23             |
| F321            | Zr3_0       | 9                | G009            | Zr4_0       | 8                |
|                 | Zr3_1       | 4.5              |                 | Zr4_1       | 4                |
|                 | Zr3_2       | 2.25             |                 | Zr4_2       | 2                |
|                 | Zr3_3       | 1.13             |                 | Zr4_3       | 1                |
|                 | Zr3_4       | 0.56             |                 | Zr4_4       | 0.5              |
|                 | Zr3_5       | 0.28             |                 | Zr3_5       | 0.25             |

where  $\Delta L^*$ ,  $\Delta a^*$  and  $\Delta b^*$  measure the differences in luminosity and in chromaticity between two colors. In this way the hue variation due to the coating step were determined.

To evaluate the effect of the coating on the tile appearance, the gloss of the samples was measured by a Novo Gloss Trio apparatus; measurements were performed by using  $60^\circ$  as standard geometry.

In order to qualitatively examine the crystalline phases developed by soluble salts, X-ray diffraction measurements (XRD) were carried out on the samples using a conventional Bragg–Brentano diffractometer (X'PERT PRO, Philips Research Laboratories) with Ni-filtered Cu  $K\alpha$  radiation. The patterns were recorded in the  $5\text{--}80^\circ$   $2\theta$  range at room temperature, with a scanning rate of  $0.001^\circ/\text{s}$  and a step size of  $0.02^\circ$ . To verify the influence of soluble salts applications on scratch resistance, scratch tests (Micro-Combi tester) with linearly increasing load (0.1–30 N, scratch speed of 1 mm/min) were performed on the samples using a Rockwell indenter with spherical tip, 100  $\mu\text{m}$  radius. At least, three scratches were performed on each coating, with the minimum distance between two scratches set at 4 mm to achieve results representative of the average response over greater surfaces. The critical loads

$L_{c1}$  (first crack) and  $L_{c2}$  (edge spallation) were determined by optical microscopy. Finally, the microstructure of the samples was investigated by scanning electron microscopy (SEM) using a XL 30 instrument (Philips) coupled with an energy dispersion spectroscopy (EDS, INCA) equipment over gold-coated samples.

### 3. Results and discussion

Sintering degree was studied in terms of linear shrinkage (LS%) and water absorption (WA%) as a function of applied solution concentration. The obtained results, from a technological point of view, assure that the proposed treatment is compatible with the industrial production. In particular, the water absorption, strictly related to the material microstructure and to the open porosity, significantly decreases (from 0.28 to 0.16%), independently to the counter ion present in solution, as the zirconium concentration is increased with respect to the commercial material (0.3%). This behavior is also confirmed by the microstructural analysis of surfaces. In general, in fact, the surface had a higher sinterisation degree as the utilized solution is concentrated (Fig. 1). The figure clearly showed that Zr1.0 sample has an higher compaction

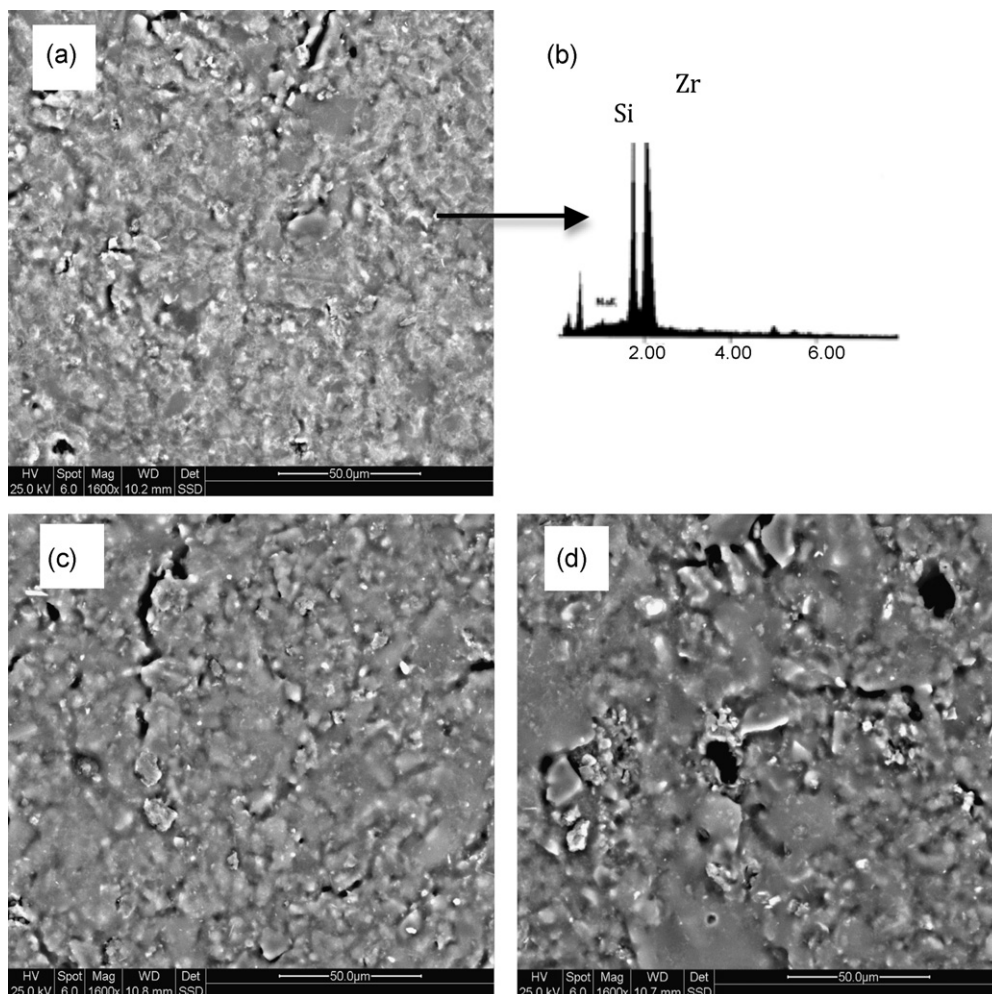


Fig. 1. SEM micrographs of Zr1.0 (a), Zr1.5 (c) and untreated tile (d) surfaces. EDS spectra (b) of white crystals in Zr1.0 samples.

Table 2  
 $\Delta E^*$  and gloss values of the prepared coatings.

| Sample code | $\Delta E^*$ | Gloss (GU)      | Sample code | $\Delta E^*$ | Gloss (GU)      |
|-------------|--------------|-----------------|-------------|--------------|-----------------|
| Zr1_0       | 1.16         | $5.40 \pm 0.44$ | Zr2_0       | 1.40         | $5.02 \pm 0.13$ |
| Zr1_1       | 0.94         | $5.70 \pm 0.12$ | Zr2_1       | 0.83         | $4.86 \pm 0.05$ |
| Zr1_2       | 0.38         | $4.90 \pm 0.14$ | Zr2_2       | 0.72         | $4.96 \pm 0.09$ |
| Zr1_3       | 0.32         | $4.72 \pm 0.16$ | Zr2_3       | 0.86         | $4.92 \pm 0.08$ |
| Zr1_4       | 0.27         | $4.74 \pm 0.11$ | Zr2_4       | 0.43         | $4.66 \pm 0.24$ |
| Zr1_5       | 0.35         | $4.80 \pm 0.10$ | Zr2_5       | 0.44         | $4.62 \pm 0.08$ |
| Zr3_0       | 3.83         | $4.06 \pm 0.05$ | Zr4_0       | 2.69         | $4.82 \pm 0.04$ |
| Zr3_1       | 1.98         | $4.50 \pm 0.07$ | Zr4_1       | 1.00         | $4.86 \pm 0.05$ |
| Zr3_2       | 1.63         | $4.62 \pm 0.35$ | Zr4_2       | 0.96         | $5.04 \pm 0.21$ |
| Zr3_3       | 0.90         | $4.84 \pm 0.05$ | Zr4_3       | 0.94         | $4.88 \pm 0.04$ |
| Zr3_4       | 0.86         | $4.56 \pm 0.29$ | Zr4_4       | 0.90         | $4.82 \pm 0.04$ |
| Zr3_5       | 0.92         | $4.68 \pm 0.13$ | Zr4_5       | 0.89         | $4.86 \pm 0.05$ |

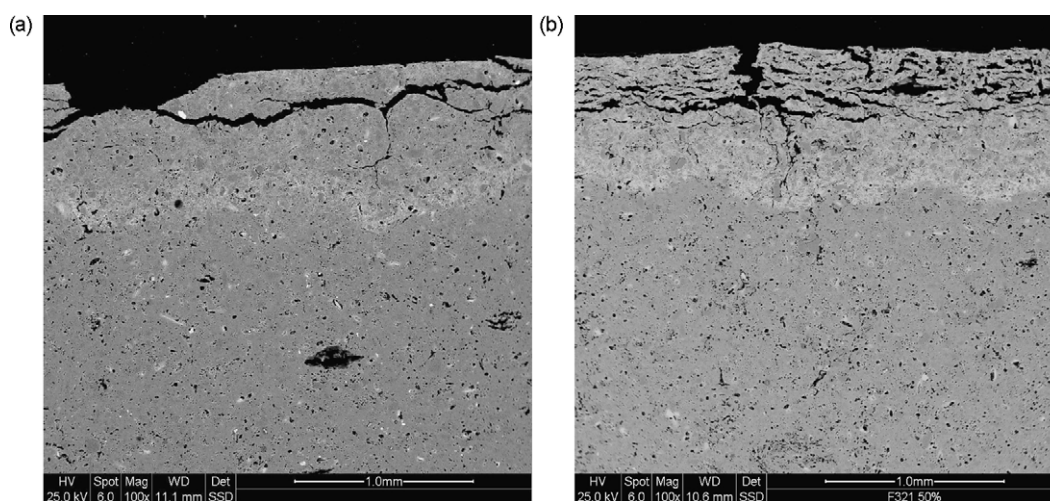


Fig. 2. SEM images of the cross-sections of Zr1\_0 and Zr3\_1 samples.

while the Zr1\_5 sample has a surface comparable with that of untreated tile. Moreover, the images clearly show as the presence of white crystals, that can be attributed to zirconia phase as underlined by EDS spectra, decreases as the dilution is increased.

In Table 2,  $\Delta E^*$  between the treated tile surfaces and the untreated tile surface are reported. The table clearly shows that in general the value is  $>1$  with the as received solution (ZrX\_0). As the dilution is increased,  $\Delta E^*$  decreases indicating that there is not a visible hue variation due to the solutions application with respect to the untreated tile. This result underlines that the zirconia nanoparticles are well dispersed in the matrix. A different behavior is observed in Zr3 samples where the  $\Delta E^*$  values are higher than 1 up to the Zr3\_2 sample. This behavior is due to the lower penetration rate of this solution for higher concentrations. In Fig. 2 the SEM micrographs obtained on the cross-section of Zr1\_0 and Zr3\_1 samples underlined that in these cases the zirconia particles were confined very close to the surface allowing to internal strain and thus to the superficial crack of the samples.

In Table 2, the gloss measured on the prepared samples is also reported. This parameter that is correlated to the surface roughness of the samples is always slightly lower than that of untreated surface ( $5.30 \pm 0.14$  GU) indicating that the deposited

solutions do not extensively modify the roughness of the samples, in agreement with the images reported in Fig. 1.

In order to qualitatively examine the crystalline phases developed by the soluble salts, X-ray diffraction measurements (XRD) were carried out on the samples (Fig. 3). The figure

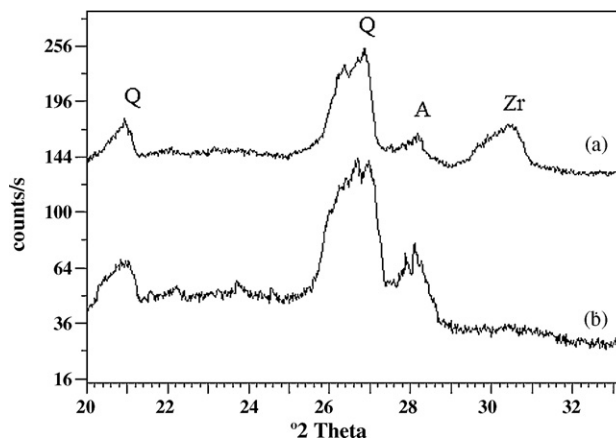


Fig. 3. XRD patterns of Zr1\_1 sample (a) in comparison with that of untreated sample (b). Q = quartz; A = anorthite; Z = t-zirconia.



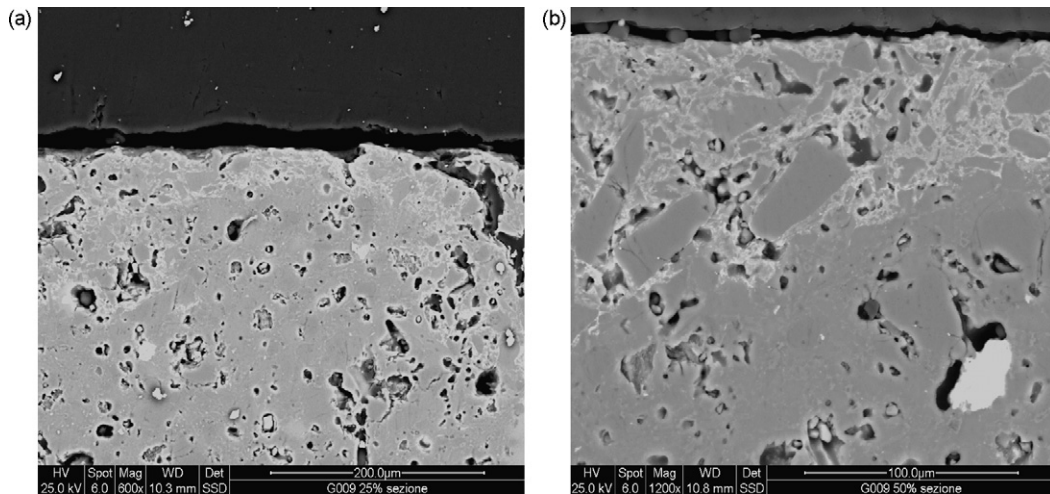


Fig. 4. SEM images of the cross-sections of Zr4.1 sample.

clearly showed that in the treated samples tetragonal zirconia phase (ICDD #00-017-923) is present. This metastable phase is probably stabilized by the nanometric dimension of particles<sup>15</sup> or by CaO presents in the matrix.

To verify the effect of zirconia nanoparticles on scratch resistance, scratch tests with linearly increasing load were performed on the samples. In Table 3 the critical load values are reported for the obtained samples. In this characterization the ZrX\_0 and Zr3\_1 and Zr3\_2 samples were eliminated for the superficial defects previously determined. Regarding the as obtained samples, only the  $L_{C2}$  values are reported because the roughness of the surfaces does not allow to determine the  $L_{C1}$  values. In general, as the dilution is increased  $L_{C2}$  decreases indicating a direct correlation with the superficial mechanical properties. In fact, a

higher dilution allows to an higher penetration with zirconia particles that do not crystallized on the surface. In particular, Zr1\_1 sample has the higher value (10.0 N) with an increase of 22% with respect of untreated sample (7.8 N). Finally, the Zr4 solution does not allow, even at higher concentration, to an increase of the mechanical properties.

Regarding the polished samples, the table evidenced a contrary behavior. The  $L_{C1}$  and  $L_{C2}$  values increase as the dilution is increased. During the polishing step, in fact, 0.5 mm of superficial layer is removed and, consequently, in the samples characterized by lower penetration and higher zirconium concentration also the zirconia particles are removed. In Fig. 4, as representative, the Zr4\_1 sample before polishing. In this sample the penetration of zirconium solution is very low and zirconia particles can be observed only up to almost 100 µm of depth.

Finally, Zr1\_4 sample has the higher  $L_{C2}$  value (5.3 N) with an increase of 36% with respect of untreated polished sample (3.5 N).

Table 3  
Second critical load ( $L_{C2}$ ) and third critical load ( $L_{C3}$ ) of the obtained samples.

| Sample code    | $L_{C2}$ (N) as obtained | $L_{C1}$ (N) | $L_{C2}$ (N) |
|----------------|--------------------------|--------------|--------------|
|                |                          | Polished     |              |
| Untreated tile | 7.8 ± 0.4                | 3.5 ± 0.2    | 8.7 ± 0.1    |
| Zr1.1          | 10.0 ± 0.2               | 4.0 ± 0.3    | 8.2 ± 0.1    |
| Zr1.2          | 9.8 ± 0.1                | 3.9 ± 0.4    | 8.0 ± 0.2    |
| Zr1.3          | 9.0 ± 0.4                | 5.1 ± 0.2    | 11.0 ± 0.5   |
| Zr1.4          | 7.2 ± 0.3                | 5.3 ± 0.3    | 11.1 ± 0.3   |
| Zr1.5          | 6.8 ± 0.7                | 4.2 ± 0.1    | 9.4 ± 0.3    |
| Zr2.1          | 9.4 ± 0.1                | 3.9 ± 0.1    | 7.7 ± 0.4    |
| Zr2.2          | 9.3 ± 0.1                | 4.1 ± 0.2    | 7.9 ± 0.5    |
| Zr2.3          | 7.0 ± 0.4                | 4.2 ± 0.1    | 7.7 ± 0.3    |
| Zr2.4          | 7.2 ± 0.5                | 4.6 ± 0.2    | 10.6 ± 0.2   |
| Zr2.5          | 5.5 ± 0.3                | 3.6 ± 0.5    | 7.2.0 ± 0.1  |
| Zr3.3          | 8.6 ± 0.4                | 4.2 ± 0.2    | 8.2 ± 0.3    |
| Zr3.4          | 8.6 ± 0.5                | 4.8 ± 0.3    | 9.1 ± 0.2    |
| Zr3.5          | 7.6 ± 0.5                | 3.8 ± 0.5    | 8.9 ± 0.4    |
| Zr4.1          | 7.2 ± 0.2                | 3.9 ± 0.4    | 8.6 ± 0.5    |
| Zr4.2          | 7.0 ± 0.3                | 4.0 ± 0.3    | 8.4 ± 0.4    |
| Zr4.3          | 6.2 ± 0.1                | 4.0 ± 0.4    | 9.1 ± 0.1    |
| Zr4.4          | 5.8 ± 0.5                | 4.4 ± 0.6    | 9.5 ± 0.1    |
| Zr4.5          | 5.8 ± 0.3                | 4.4 ± 0.1    | 9.4 ± 0.6    |

#### 4. Conclusion

The obtained results show that the scratch resistance generally increases by the addition of zirconium soluble salts. The increasing, however, significantly depends on the counter ion present in solution that directly affects the penetration ability of the zirconium solution. In particular, both in as fired and in polished samples, the Zr1 solution, in the optimized dilution (Zr1\_1 and Zr1\_2), seem to allow to the higher improve of mechanical properties.

#### Acknowledgements

Support from Prin2007 project “Made in Italy in the ceramic industry for building use. Nanopowders and nanotechnologies for the aesthetic innovation and functionalization of the ceramic surfaces” (20073MZALE) and experimental help of Dr. Alessandro Ferrari are gratefully acknowledged.

## References

1. FINE PORCELAINIZED STONEWARE, ed. SACMI in web site [www.sacmi.com](http://www.sacmi.com).
2. Manfredini, T., Pellacani, G. C., Romagnoli, M. and Pennisi, L., Porcelainized stoneware tiles. *Am Ceram Soc Bull*, 1995, **74**, 76.
3. Leonelli, C., Bondioli, F., Veronesi, P., Romagnoli, M., Manfredini, T., Pellacani, G. C. et al., Enhancing the mechanical properties of porcelain stoneware tiles—a microstructural approach. *J Euro Ceram Soc*, 2001, **21**, 785.
4. Barthlott, W. and Neinhuis, C., The purity of sacred lotus or escape from contamination in biological surfaces. *Planta*, 1997, **202**, 1.
5. Kuisma, R., Fröberg, L., Kymäläinen, H., Pesonen-Leinonen, E., Piispanen, M., Melamies, P. et al., Topography and cleanability of uncoated and fluoropolymer, zirconia and titania coated ceramic glazed surfaces. *J Euro Ceram Soc*, 2007, **27**, 101.
6. Watson, G. S. and Watson, J. A., Natural nano-structures on insects—possible functions of ordered arrays characterized by atomic force microscopy. *Appl Surf Sci*, 2004, **235**, 139.
7. Wang, R., Hashimoto, K., Fujishima, A., Chikuni, M., Kojima, E., Kitamura, A. et al., Light-induced amphiphilic surfaces. *Nature*, 1997, **388**, 431.
8. Fujishima, A., Rao, T. N. and Tryk, D. A., Titanium dioxide photocatalyst. *J Photochem Photobiol*, 2000, **C1**, 1.
9. Fujishima, A., Rao, T. N. and Tryk, D. A., TiO<sub>2</sub> photocatalysts and diamond electrodes. *Electrochim Acta*, 2000, **45**, 4683.
10. Benedix, R., Dehn, F., Quaas, J. and Orgass, M., Application of titanium dioxide photocatalysis to create self-cleaning building materials. *Lacer*, 2000, **5**, 157.
11. Bondioli, F., Taurino, R. and Ferrari, A. M., Functionalization of ceramic tile surface by sol–gel technique. *J Colloid Interface Sci*, 2009, **334**, 195–201.
12. Taurino, R., Fabbri, E., Messori, M., Pilati, F., Pospieck, D. and Syntaska, A., Facile preparation of superhydrophobic coatings by sol–gel processes. *J Colloid Interface Sci*, 2008, **325**, 149.
13. CIE, Recommendations of Uniform Color Spaces, Color Difference Equations, Phychometrics Color Terms, Supplement No. 2 of CIE Publ. no. 15 (E1-1.31) 1971, Bureau Central de la CIE, Paris, 1978.
14. Hunter, R. S., Photoelectric color difference meter. *J Opt Soc Am*, 1958, **48**, 985.
15. Garvie, R. C., The occurrence of metastable tetragonal zirconia as crystallite size effect. *J Phys Chem*, 1965, **69**(4), 1238.